

# An investigation on the formation mechanism of nano ZrB<sub>2</sub> powder by a magnesiothermic reaction

M. Jalaly<sup>1,\*</sup>, M.Sh. Bafghi<sup>1</sup>, M. Tamizifar<sup>1</sup>, F.J. Gotor<sup>2</sup>

1. School of Metallurgy and Materials Engineering, Iran University of Science & Technology  
(IUST), Narmak, Tehran 16846-13114, Iran

2. Instituto de Ciencia de Materiales de Sevilla, Americo Vespucio 49, 41092 Sevilla, Spain

\*Corresponding Author, Email: [maisam\\_jalaly@iust.ac.ir](mailto:maisam_jalaly@iust.ac.ir)

Tel: +989127387902, Fax: +982177240480

## Abstract

Nanocrystalline zirconium diboride (ZrB<sub>2</sub>) powder was produced by magnesiothermic reduction in the Mg/ZrO<sub>2</sub>/B<sub>2</sub>O<sub>3</sub> system. In this study, high-energy ball milling was used to generate the essential conditions to induce a mechanically induced self-sustaining reaction (MSR). The ignition time for ZrB<sub>2</sub> formation was found to be approximately 6 minutes. The mechanism for the formation of ZrB<sub>2</sub> in this system was determined by studying the relevant sub-reactions, the effect of stoichiometry, and the thermal behavior of the system.

**Keywords:** Zirconium diboride; Mechanosynthesis; Formation mechanism.

## 1. Introduction

Diborides of group IV-B transition metals (TiB<sub>2</sub>, ZrB<sub>2</sub>, and HfB<sub>2</sub>) have been found to be a suitable class of materials for use in ultra-high temperature ceramics [1]. The distinctive features of these materials make them appropriate for use in various high temperature applications, such as hypersonic flights, atmospheric re-entry vehicles, and

rocket propulsion systems. Zirconium diboride has attracted the most attention because of its superior oxidation resistance, which is a consequence of the stability of the  $ZrO_2$  layer that is formed on these materials at high temperatures in oxidizing atmospheres [2].

The refractoriness and high stability of transition metal diborides are due to the high negative Gibbs free energy of formation, which is strongly correlated to the formation enthalpy. Therefore, an appropriate reaction can be selected for the synthesis of these compounds by means of inducing a highly exothermic self-sustaining reaction. For instance,  $TiB_2$ ,  $ZrB_2$ , and  $HfB_2$  have been obtained by self-propagating high-temperature synthesis (SHS) from their constituent elements [3–6]. This type of synthesis is characterized by its significant negative enthalpy and high adiabatic temperature ( $T_{ad}$ ) of greater than 1800 K [7].  $ZrB_2$  has also been obtained through several other reactions, including the borothermic reduction of  $ZrO_2$  [8,9], the carbothermic reduction of  $ZrO_2$  and  $B_2O_3$  [10,11], and the reduction of  $ZrO_2$  by boron carbide [12-14]. However, a literature survey revealed that the metallothermic reduction of  $ZrO_2$  and  $B_2O_3$  has been producing the most interest due to its inexpensive raw materials as well as the high exothermic nature of the relevant self-sustainable reactions [15-21]. Although aluminum has been chosen in a few cases to reduce zirconium and boron oxides [20,21], magnesium appears to be more attractive for reducing these oxides [15-19] because of the feasibility of MgO leaching.

Mechanochemical processes can be referred to as mechanically induced self-sustaining reactions (MSR) [7] when an SHS reaction is induced by the high-energy ball milling of the reactants after the completion of a critical milling period, called the ignition time. In contrast to the conventional SHS procedure, the MSR process has the

side benefit of performing the following in a single step: the mixing of the reactants, the subsequent homogenization of the products, and the extreme particle size reduction of both reactants and products.

The synthesis of  $ZrB_2$  using high-energy ball milling has been examined by a number of researchers. Setoudeh and Welham [17] studied the formation of  $ZrB_2$  by conducting the magnesiothermic reduction by means of milling, using  $ZrO_2$  and  $B_2O_3$  as the sources of Zr and B, respectively. In that study, no MSR process was observed and the  $ZrB_2$  was synthesized after 15 hours of milling, which is comparable to a normal mechanical alloying process. Akgun et al. [19] also attempted to produce zirconium diboride by mechanochemical treatment of  $ZrO_2$ - $B_2O_3$ -Mg. In their study, zirconium diboride was obtained after 30 hours of milling, indicating that no MSR reaction occurred, most likely due to the low milling intensity regime used in their experiments.

The primary goal of the present work, therefore, was to investigate the mechanosynthesis of  $ZrB_2$  powder, using  $ZrO_2$  and  $B_2O_3$  as starting materials, through the first demonstration of a mechanically induced self-sustaining reaction of magnesiothermic reduction. Another significant goal of this study was to understand the mechanisms involved in the  $ZrB_2$  formation process in this system by studying the sub-reactions as well as the influence of the stoichiometry of the reactants.

## **2. Material and methods**

Zirconium diboride samples were produced by using stoichiometric amounts of monoclinic  $ZrO_2$  (99%, Aldrich, St. Louis, MO),  $B_2O_3$  (98%, Fluka, St. Louis, MO), and Mg (99%, Riedel-de Haën, Seelze, Germany) powders. The starting materials were ball-milled in a modified planetary ball mill (Pulverisette7, Fritsch, Idar-Oberstein,

Germany) under an argon atmosphere. The rotational speed and ball-to-powder mass ratio were 600 rpm and 30:1, respectively. The milling vial and balls (15 mm) were made of hardened chromium steel. All the milling experiments were conducted under high-purity argon gas at a pressure of 5 bar. The vial was purged with argon gas several times, and the desired pressure was adjusted before the start of the milling. The connection of the vial to the gas cylinder during the milling experiments was maintained by a rotating union (model 1005-163-038; Deublin, Waukegan, IL) and a flexible polyamide tube. The pressure changes vs. time were monitored by a SMC solenoid valve (model EVT307-5DO-01F-Q, SMC Co., Tokyo, Japan) to record the ignition time. A sharp peak due to the pressure rise appears when the MSR reaction occurs. The position of this peak indicates the ignition time. The system used in this work has already been shown elsewhere [22]. The magnesium oxide by-product was removed by leaching the as-milled powder in 1 M HCl at 80 °C for 1 h.

The thermal behavior of the as-received powders was studied by differential scanning calorimetry (DSC) in a TA Instrument Q600 (New Castle, DE) using a constant heating rate of 10 °C/min from room temperature to 1400 °C. The DSC measurements were performed under a flowing helium atmosphere. Furthermore, isothermal annealing of the powders was performed at different temperatures for 30 min under a flowing argon atmosphere at a pressure of 1 bar in a horizontal tube furnace (IGM1360 model no. RTH-180-50-1H, AGNI, Aachen, Germany).

The samples were investigated using X-ray diffraction (XRD) analysis to determine the structural changes of the powders during the milling and heating experiments. A PANalytical X'Pert diffractometer (Almelo, the Netherlands) (45 kV, 40 mA) with Cu K<sub>α</sub> radiation ( $\lambda = 0.15406$  nm) was used for the XRD analysis. The

crystallite size of the sample was estimated by the peak-broadening analysis of the XRD peaks using the Williamson–Hall formula [23].

Scanning electron microscopy (SEM) images were obtained using a Hitachi S-4800 SEM-Field Emission microscope (Tokyo, Japan). Transmission electron microscopy (TEM) images were obtained using a 200 kV CM200 microscope (FEI, Hillsboro, OR) equipped with a SuperTwin objective lens and a tungsten filament (point resolution  $\varnothing = 0.25$  nm). To prepare samples for TEM imaging, the powdered samples were dispersed in ethanol, and droplets of the suspension were deposited onto holey carbon films.

### 3. Results and Discussion

#### 3.1. Mechanochemistry

The first goal of this work was to synthesize the zirconium diboride compound. To achieve this goal, the following reaction was considered:



$$\Delta G^\circ_{298} = -931 \text{ kJ}, \Delta H^\circ_{298} = -960 \text{ kJ}, T_{\text{ad}} \approx 2900 \text{ K}$$

Stoichiometric amounts of the starting materials were subjected to milling under the aforementioned conditions. The gas pressure change inside the vial versus the milling time is shown in Fig. 1. A large pressure increase was observed at approximately 6 min of milling, indicating that the MSR reaction, a significant exothermic reaction, occurred and that the ignition time was approximately 6 min.

The XRD patterns of the Mg, ZrO<sub>2</sub>, and B<sub>2</sub>O<sub>3</sub> powder mixture as-blended and after different milling times as well as of the leached sample are shown in Fig. 2. The XRD pattern of the as-blended mixture exhibited only the sharp peaks of Mg (ICDD

PDF #35-0821),  $\text{ZrO}_2$  (ICDD PDF #13-0307), and  $\text{B}_2\text{O}_3$  (ICDD PDF #06-0297). The sharp peaks from the products of reaction 1,  $\text{ZrB}_2$  (ICDD PDF #34-0423) and  $\text{MgO}$  (ICDD PDF #45-0946), were observed after 6 min of milling, although traces of Mg and  $\text{ZrO}_2$  were still observed. The observation of trace levels of the reactants is a typical behavior in mechanochemical reactions, especially in MSR situations [21], due to the entrapment of some powder in the dead zones of the milling vial at early times. As shown in Fig. 2, a tetragonal  $\text{ZrO}_2$  phase (nominated as T- $\text{ZrO}_2$ ) was detected among the remaining materials in the sample that was milled for 6 min (the ignition point). In fact, it appears that a portion of the initial monoclinic zirconia transformed into the tetragonal form due to the significant increase of temperature caused by the highly exothermic MSR reaction. As shown in Fig. 2, a trace amount of elemental Zr was observed in the XRD pattern for the sample after 6 min of milling, which is most likely due to the reduction of zirconia. By increasing the milling time, the unprocessed powders are eventually subjected to the ball incidences, thus gaining sufficient energy to be locally reacted. As shown in Fig. 1, no further peak in pressure was observed after 6 min, indicating that the amount of unreacted agglomerates and/or entrapped particles is negligibly small. Thus the particles can be reacted locally to complete the reaction, but the temperature and pressure do not increase noticeably. Fig. 2 also presents the XRD patterns of the samples that were milled for 2 and 3 hours. Although a slight amount of zirconium dioxide can be observed after 2 h of milling, it is obvious that the peaks of the remaining Mg and  $\text{ZrO}_2$  disappeared completely after 3 h of milling. The corresponding peaks of  $\text{ZrB}_2$  and  $\text{MgO}$  were broadened, and their intensities gradually reduced during the long-term ball milling process, indicating the introduction of lattice defects into the crystal structures and the decrease of the grain size of the products into

the nanoscale regime. The crystallite size of  $\text{ZrB}_2$  after 3 h of the ball milling process was calculated to be approximately 56 nm. Dissolution of the magnesium oxide by-product was performed using 1 M HCl. The XRD traces of the leached product after 3 h milling are shown in Fig. 2. Although a very small peak at approximately  $31^\circ$  corresponds to unreacted  $\text{ZrO}_2$ , no magnesium oxide was observed, and the major phase after leaching was  $\text{ZrB}_2$ . The trace amount of residual  $\text{ZrO}_2$  has been reported in various processes by several researchers [14, 16, 18] due to its high chemical stability.

It is noteworthy that there are some research [17, 19] in the literature dealt with synthesis of  $\text{ZrB}_2$  by the magnesiothermic reduction of  $\text{ZrO}_2$  and  $\text{B}_2\text{O}_3$  through high energy milling. Compared to the short ignition time (6 min) obtained in the present work,  $\text{ZrB}_2$  was prepared gradually (not in a self-sustaining manner) in the these works after long milling times of 15 h [17] and 30 h [19]. The main difference between the present research and these works lies in the intensity of milling process. A tumbling mill at a rotational speed of 165 rpm and a planetary mill at 300 rpm were used in [17] and [19], respectively, while the high speed of 600 rpm was applied in the present work. Therefore, this can provide an example of the efficient role of the experimental conditions in the development of a self-sustaining reaction [7].

The SEM and TEM micrographs of a sample milled for 3 h are shown in Fig. 3. Flattened agglomerates are shown in the SEM micrograph in Fig. 3 (a) that are composed of semi-spherical particles of sub-micrometric and nanometric sizes. The TEM micrograph in Fig. 3 (b) shows nanoparticles of hexagonal  $\text{ZrB}_2$  single crystals (Z area) and of magnesium oxide (M area).

### **3.2. Mechanism of product formation**

### 3.2.1. During milling

The mechanism for the formation of  $ZrB_2$  during milling in the present system can be described as follows. Zirconium and boron oxides must be reduced to their corresponding elements to form zirconium diboride. These sub-reactions are as follows:



$$\Delta G^\circ_{298} = -515 \text{ kJ}, \Delta H^\circ_{298} = -532 \text{ kJ}, T_{ad} \approx 2630 \text{ K}$$



$$\Delta G^\circ_{298} = -98 \text{ kJ}, \Delta H^\circ_{298} = -107 \text{ kJ}, T_{ad} \approx 1070 \text{ K}$$



$$\Delta G^\circ_{298} = -318 \text{ kJ}, \Delta H^\circ_{298} = -322 \text{ kJ}, T_{ad} \approx 3200 \text{ K}$$

Regarding the adiabatic temperatures ( $T_{ad}$ ) and enthalpies of the above system, reactions 2 and 4 possess the necessary conditions to satisfy the Merzhanov criterion [7] to proceed in an SHS or MSR manner. However, the reduction of  $ZrO_2$  by Mg (reaction 3) does not satisfy this condition, and it is hence expected to gradually proceed as an ordinary reaction.

When Mg,  $B_2O_3$ , and  $ZrO_2$  are concurrently present in one system, Mg reduces boron oxide in a self-sustaining manner to yield elemental boron together with the generation of a significant amount of heat; this heat increases the system temperature inside the milling vial to a level that can initiate the reaction between Mg and zirconia to form elemental Zr. As a result,  $ZrB_2$  can be synthesized by the reaction between these two reduced elements. The highly exothermic reaction of the reduced B and Zr (reaction 4) can provide an extra amount of heat to the system, thus enabling the further reduction of  $ZrO_2$  to proceed more easily. These three reactions occur simultaneously; therefore,

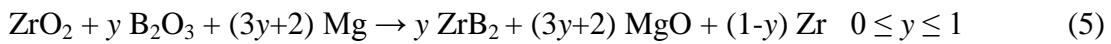


only one peak is observed in the pressure-time diagram of the total reaction (1). This proposed reaction mechanism is supported by the presence of a trace amount of residual zirconium in the XRD pattern just after the ignition time.

To examine the proposed mechanism, the sub-reactions were individually investigated. Stoichiometric amounts of Mg/B<sub>2</sub>O<sub>3</sub>, Mg/ZrO<sub>2</sub>, and Zr/B were mixed according to reactions 2 to 4 and milled under the same conditions. For reaction 2, the ignition time obtained from the related pressure-time graph (Fig. 4) was found to be approximately 8 min. This ignition time is slightly longer than the ignition time of reaction 1 due to the lower exothermicity of reaction 2. The XRD patterns of the initial mixture along with the milled sample up to the ignition point (8 min) are shown in Fig. 5. The ignited sample is observed to contain magnesium oxide and trace amounts of the starting magnesium, which remained unreacted due to its entrapment in the dead zones inside the vial, as mentioned above. Elemental boron cannot be observed in the pattern, most likely due to its amorphous state. A small amount of a MgO-rich spinel (3MgO.B<sub>2</sub>O<sub>3</sub>) was also formed after ignition. The formation of this type of spinel phase can be explained as a consequence of the reaction between the increased amount of MgO (being the reaction product) and the reduced amount of the remaining boron oxide. For reaction 3, as expected from its thermodynamic data, no pressure increase was observed throughout the milling process. Fig. 6 shows the XRD patterns of the unmilled and milled powders for milling times of up to 4 h in this system. Only XRD peak broadening was observed, with no sign of the occurrence of any reaction during this long milling time. These XRD data indicate that Mg cannot reduce zirconia under the prevailing conditions during this time period. This reaction can occur in a gradual manner (i.e., non-self-sustaining mode) under more extreme, intensive conditions for a

much longer time. In the case of reaction 4, the ignition time was approximately 17 min, as shown in Fig. 4. The longer ignition time in this system compared to reactions 1 and 2 may be attributed to its less exothermic nature. The XRD results in Fig. 7 indicate that ZrB<sub>2</sub> was completely synthesized after the ignition time of 17 min. In summary, the individual study of these sub-systems confirms that the ZrB<sub>2</sub>-MgO composite in reaction 1 was produced through the proposed mechanism.

As previously mentioned, the overall reaction (1), which is a self-sustaining reaction, is composed of two self-sustaining reactions (reactions 2 and 4) and one non-self-sustaining reaction (reaction 3). According to the previously proposed mechanism, B and Zr must be produced to form ZrB<sub>2</sub>. However, the reduction reaction for boron is not fundamentally similar to the reduction reaction for zirconium. Therefore, it would be interesting to understand how this transition from a non-self-sustaining reaction to a self-sustaining reaction is achieved. To examine this phenomenon, the following general reaction was developed:



where the amount of B<sub>2</sub>O<sub>3</sub> is considered as a variable. Once B<sub>2</sub>O<sub>3</sub> is added to the binary ZrO<sub>2</sub>-Mg system (non-self-sustaining reaction 3), it can be reduced to boron by magnesium, and the heat generated causes zirconia to be reduced to zirconium. Subsequently, the total amount of boron and the stoichiometric portion of the reduced zirconium react to form ZrB<sub>2</sub>, and the remaining zirconium remains as an elemental product. When y is equal to zero, reaction 5 converts to reaction 3, which is a non-self-sustaining reaction. When y is equal to one, reaction 5 changes to reaction 1, which is a self-sustaining reaction. These two extremes in the types of reactions imply that there is a transition point between these extremes that occurs with the addition of boron oxide to

zirconium oxide, in which the reaction transforms from one of a gradual nature to one of a self-sustaining nature. Therefore, the amount of  $B_2O_3$  is expected to be a critical parameter.

If the adiabatic temperature ( $T_{ad}$ ) is considered to be a measure of the self-sustaining tendency, this transition can be illustrated by plotting  $T_{ad}$  of reaction 5 versus the  $y$  values. Fig. 8 shows the thermodynamic calculations for  $T_{ad}$  and the room temperature enthalpy of reaction 5 for various compositions with  $y$  in the range between 0 and 1 in intervals of 0.1. As  $y$  increases, the enthalpy of the reaction clearly becomes more negative, resulting in more suitable thermodynamic conditions for the reaction to occur. Because a reaction requires  $T_{ad}$  to be at least 1800 K to become self-sustaining (known as the Merzhanov criterion) [21], it can be observed from Fig. 8 that the compositions with  $y \geq 0.3$  should theoretically behave in the self-sustaining manner. In other words, in the case of compositions with  $0 \leq y < 0.3$ , the amount of boron oxide is not sufficient to release enough heat by magnesiothermic reduction to induce the entire system to become self-sustaining. For compositions with  $y \geq 0.3$ , the amount of  $B_2O_3$  is sufficient to be reduced in a self-sustaining manner by Mg and to simultaneously enable  $ZrO_2$  to be reduced to Zr.

To verify this thermodynamic hypothesis, typical compositions with different  $y$  values between 0 and 1 in intervals of 0.1 were processed by high energy ball milling to induce MSR reactions. From the XRD results in Fig. 9, the compositions with  $y \geq 0.6$  were observed to behave in a self-sustaining manner, and the expected products of reaction 5 were completely formed after the ignition point of 6 min (the result corresponding to  $y = 1$  is shown in Fig. 2). However, no ignition occurred for compositions with  $y < 0.6$ , even after a long milling time. As an example of the lack of

ignition, the XRD pattern for the sample with  $y = 0.5$  composition after 2 h of milling is shown in Fig. 9. Consequently, the theory for the transition from the gradual reaction mode to the self-sustaining reaction mode in this system appears to be valid, although there is a difference between the thermodynamically calculated and experimentally observed criterion in the range of  $y = 0.3$ – $0.6$ . The main reason of the difference is supposed to be related to the kinetic aspects of the reaction rather than thermodynamic ones. For this range, a self-sustaining reaction is thermodynamically possible, but the experimental conditions applied in the present work were not energetic enough to stimulate the reacting materials to be reduced in a self-sustaining manner. It seems that by decreasing the  $B_2O_3$  fraction, the amount of boron oxide in this range has not been sufficient to provide adequate energy to overcome the activation energy of the system. Thus, for  $0.3 \leq y < 0.6$ , the overall reaction is expected to become self-sustaining if additional external energy is given to the system by more intense milling conditions. This postulation was previously proved by the authors in the case of  $ZrSiO_4/B_2O_3/Mg/C$  system [24], where was shown that an increase in the rotational speed of milling caused the reaction to become self-sustaining.

### 3.2.2. Thermal analysis

Differential scanning calorimetry (DSC) was utilized to study the reaction mechanism during heating. For this purpose, a homogeneously blended  $Mg/ZrO_2/B_2O_3$  powder mixture was subjected to DSC analysis at a heating rate of  $10\text{ }^\circ\text{C}/\text{min}$ , as shown in Fig. 10. The DSC curve exhibits three endothermic peaks at approximately  $100\text{ }^\circ\text{C}$ ,  $180\text{ }^\circ\text{C}$ , and  $650\text{ }^\circ\text{C}$  and two major exothermic peaks at approximately  $640\text{ }^\circ\text{C}$  and  $850\text{ }^\circ\text{C}$ . The two low-temperature endotherms appear to be related to the vaporization of water

that is physically and chemically adsorbed to the boron oxide. The reaction between the materials clearly starts with an onset temperature of 640°C. An endotherm was also observed at 650°C, which is due to the melting of residual magnesium, indicating that the entire SHS reaction does not instantaneously occur during heating. Fig. 11 shows the XRD patterns of the products after the heating of the initial mixture at different temperatures, with the aim of clarifying the nature of the peaks that appeared in the DSC data. The XRD pattern corresponding to the annealed sample at 600°C shown in Fig. 11 indicates the presence of only the starting materials, confirming the attribution of the two low-temperature endotherms to water vaporization.

The XRD pattern obtained after the first exotherm (750°C) is shown in Fig. 11. A considerable amount of the MgO phase was observed to be formed along with unreacted initial materials with lower intensities compared to the XRD pattern of the sample heated at 600°C (especially in the case of the magnesium peaks). This formation of the MgO phase indicates that the first exotherm appearing at 640°C is related to the reduction of boron oxide by magnesium (reaction 2). In fact, the stoichiometric amount of magnesium reacts with B<sub>2</sub>O<sub>3</sub> in an SHS manner to form MgO, and the remainder of the Mg remains unreacted alongside zirconium oxide. This residual Mg melts at the melting point of magnesium (650°C), causing a sharp endothermic peak. The narrowness of the first exotherm (compared to the second one) is a characteristic feature of a self-propagating reaction, which occurs immediately.

To clarify the nature of the second exotherm observed at 850°C, heat treatments were performed at higher temperatures. The XRD pattern corresponding to the sample heated to 1000°C in Fig. 12 indicates that a considerable amount of ZrB<sub>2</sub> was formed. This formation of ZrB<sub>2</sub> demonstrates that the second exotherm is attributed to the

initiation of the  $\text{ZrO}_2$  reduction by Mg and the reaction between Zr and B to form  $\text{ZrB}_2$ . However, the reduction of zirconium oxide is a gradual reaction (non-self-sustaining reaction), which is reflected in the broad shape of the second exotherm; thus, a significant amount of  $\text{ZrO}_2$  remained at 1000 °C. By increasing the temperature to 1200 °C and 1400 °C, the maximum temperature possible in our laboratory, the major phase in the system changes to  $\text{ZrB}_2$ , but the reduction is still incomplete. The further increase of temperature would lead to a complete reaction. A slight amount of a spinel phase ( $\text{Mg}_3\text{B}_2\text{O}_6$ ) was also formed at high temperatures.

All of the heat treatments described above resulted in the preliminary reduction of boron oxide, followed by the reduction of zirconium oxide at higher temperatures. This general trend is consistent with the mechanism proposed during the mechanochemical (milling) synthesis, with an exception that the spinel phase ( $\text{Mg}_3\text{B}_2\text{O}_6$ ) observed in the thermal treatments was not detected in the milling route. This spinel phase formation in the thermal treatments is most likely due to the sufficient time at high temperatures to produce conditions that are suitable for MgO and  $\text{B}_2\text{O}_3$  to form magnesium borate.

#### **4. Conclusions**

The high-energy ball milling technique was successfully applied for the mechanosynthesis of  $\text{ZrB}_2$  nanoparticles by means of a magnesiothermic reduction. The synthesis in  $\text{Mg}/\text{B}_2\text{O}_3/\text{ZrO}_2$  was found to be MSR in nature, with an ignition time of 6 min. Examination of the sub-reactions revealed that boron oxide is easily reduced by Mg, while Mg cannot reduce  $\text{ZrO}_2$  to Zr in a self-sustaining manner. Thus, the significant amount of heat generated through the reduction of boron oxide by Mg together with the large amount of heat released by the reaction between the reduced B

and Zr is capable of activating the reduction of  $ZrO_2$ . This mechanism was confirmed by the study of the thermal behavior of the system. The amount of boron oxide was recognized as a critical parameter for inducing the system to undergo a transition from a gradual reaction to a self-sustaining reaction.

### **Acknowledgements**

This work was supported by the Spanish government under grant No. MAT2011-22981, which was financed in part by the European Regional Development Fund of 2007-2013. We also acknowledge the Ministry of Science, Research and Technology of Iran for its support in providing a visiting scholarship for M. Jalaly.

### **References**

- [1] M.A. Aviles, J.M. Cordoba, M.J. Sayagues, F.J. Gotor, Mechanochemical synthesis of  $Ti_{1-x}Zr_xB_2$  and  $Ti_{1-x}Hf_xB_2$  solid solutions, *Ceramics International* 37 (2011) 1895–1904.
- [2] W.G. Fahrenholtz, G.E. Hilmas, Refractory Diborides of Zirconium and Hafnium, *Journal of American Ceramic Society* 90 (2007) 1347–1364.
- [3] H.E. Camurlu, F. Maglia, Preparation of nano-size  $ZrB_2$  powder by self-propagating high-temperature synthesis, *Journal of the European Ceramic Society* 29 (2009) 1501–1506.
- [4] D.D. Radev, M. marinov, Properties of titanium and zirconium diborides obtained by self propagated high-temperature synthesis, *Journal of Alloys and Compounds* 244 (1996) 48-51.

- [5] S. Nakane, T. Endo, K. Hirota, Simultaneous synthesis and densification of  $\alpha$ -Zr(N)/ZrB<sub>2</sub> composites by self-propagating high-temperature combustion under high nitrogen pressure, *Ceramics International* 35 (2009) 2145–2149.
- [6] A. Makino, C. K. Law, SHS Combustion Characteristics of Several Ceramics and Intermetallic Compounds, *Journal of American Ceramic Society* 77 (1994) 778–786.
- [7] L. Takacs, Self-sustaining reactions induced by ball milling, *Progress in Materials Science* 47 (2002) 355–414.
- [8] P. Peshev, G. Bliznakov, On the borothermic preparation of titanium, zirconium and hafnium diborides, *Journal of the Less-common metals* 14 (1968) 23-32.S.
- [9] Ran, O. Van der Biest, J. Vleugels, ZrB<sub>2</sub> Powders Synthesis by Borothermal Reduction, *Journal of American Ceramic Society* 93 (2010) 1586–1590.
- [10] A.K. Khanra, L.C. Pathak, M.M. Godkhindi, Carbothermal synthesis of zirconium diboride (ZrB<sub>2</sub>) whiskers, *Advances in Applied Ceramics* 106 (2007) 155–160.
- [11] O. Balç, D. Agaogullar, I. Duman, M.L. Ovecoglu, Carbothermal production of ZrB<sub>2</sub>–ZrO<sub>2</sub> ceramic powders from ZrO<sub>2</sub>–B<sub>2</sub>O<sub>3</sub>/B system by high-energy ball milling and annealing assisted process, *Ceramics International* 38 (2012) 2201–2207.
- [12] H. Zhao, Y. He, Z. Jin, Preparation of Zirconium Boride Powder, *Journal of American Ceramic Society* 78 (1995) 2534–2536. J
- [13] .K. Sonber, T.S.R. Ch. Murthy, C. Subramanian, S. Kumar, R.K. Fotedar, A.K. Suri, Investigations on synthesis of ZrB<sub>2</sub> and development of new composites with HfB<sub>2</sub> and TiSi<sub>2</sub>, *International Journal of Refractory Metals and Hard Materials* 29 (2011) 21–30.



- [14] W.M. Guo, G.J. Zhang, Reaction Processes and Characterization of  $ZrB_2$  Powder Prepared by Boro/Carbothermal Reduction of  $ZrO_2$  in Vacuum, *Journal of American Ceramic Society* 92 (2009) 264–267.
- [15] A.K. Khanra, L.C. Pathak, S.K. Mishra, M.M. Godkhindi, Sintering of ultrafine zirconium diboride powder prepared by modified SHS technique, *Advances in Applied Ceramics* 104 (2005) 282–284.
- [16] K. Nishiyama, T. Nakamura, S. Utsumi, H. Sakai, M. Abe, Preparation of ultrafine boride powders by metallothermic reduction method, *Journal of Physics: Conference Series* 176 (2009) 012043.
- [17] N. Setoudeh, N.J. Welham, Formation of zirconium diboride ( $ZrB_2$ ) by room temperature mechanochemical reaction between  $ZrO_2$ ,  $B_2O_3$  and Mg, *Journal of Alloys and Compounds* 420 (2006) 225–228.
- [18] S.K. Mishra, S. Das, L.C. Pathak, Defect structures in zirconium diboride powder prepared by self-propagating high-temperature synthesis, *Materials Science and Engineering A* 364 (2004) 249–255.
- [19] B. Akgun, H.E. Camurlu, Y. Topkaya, N. Sevinc, Mechanochemical and volume combustion synthesis of  $ZrB_2$ , *International Journal of Refractory Metals and Hard Materials* 29 (2011) 601–607.
- [20] S.K. Mishra, S.K. Das, V. Sherbacov, Fabrication of  $Al_2O_3$ - $ZrB_2$  in situ composite by SHS dynamic compaction: A novel approach, *Composites Science and Technology* 67 (2007) 2447–2453.
- [21] Y.B. Lee, H.C. Park, K.D. Oh, C.R. Bowen, R. Stevens, Self-propagating high-temperature synthesis of  $ZrB_2$  in the system  $ZrO_2$ - $B_2O_3$ - $Fe_2O_3$ -Al, *Journal of Materials Science Letters* 19 (2000) 469–471.

[22] F.J. Gotor, M. Achimovicova, C. Real, P. Balaz, Influence of the milling parameters on the mechanical work intensity in planetary mills, *Powder Technology* 233 (2013) 1–7.

[23] G. K. Williamson, W. H. Hall, X-ray line broadening from filed aluminium and wolfram, *Acta Metallurgica* 1 (1953) 22-31.

[24] M. Jalaly, M. Tamizifar, M.Sh. Bafghi, F.J. Gotor, Mechanochemical synthesis of  $ZrB_2$ - $SiC$ - $ZrC$  nanocomposite powder by metallothermic reduction of zircon, *Journal of Alloys and Compounds* 581 (2013) 782–787.

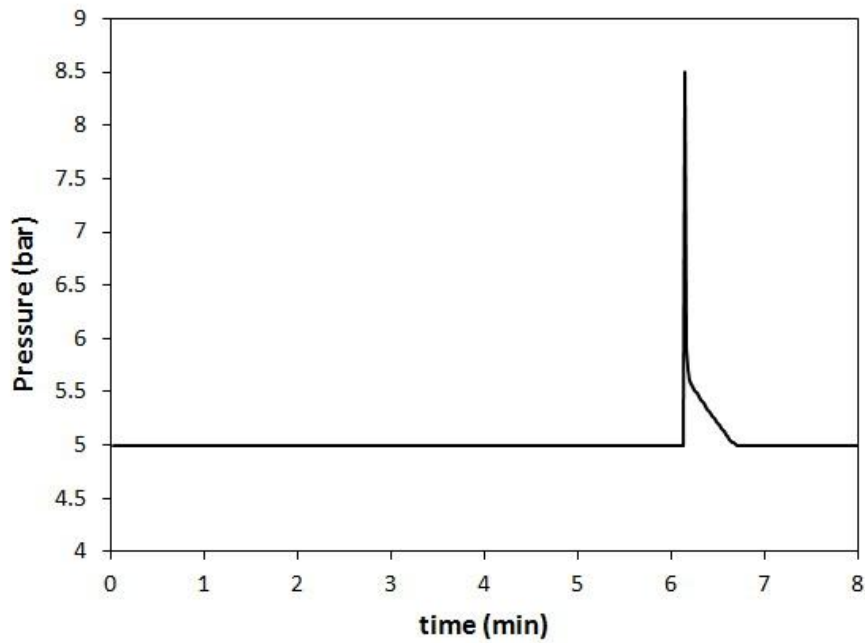


Fig. 1. Gas pressure inside the vial versus the milling time for the  $Mg/ZrO_2/B_2O_3$  system.

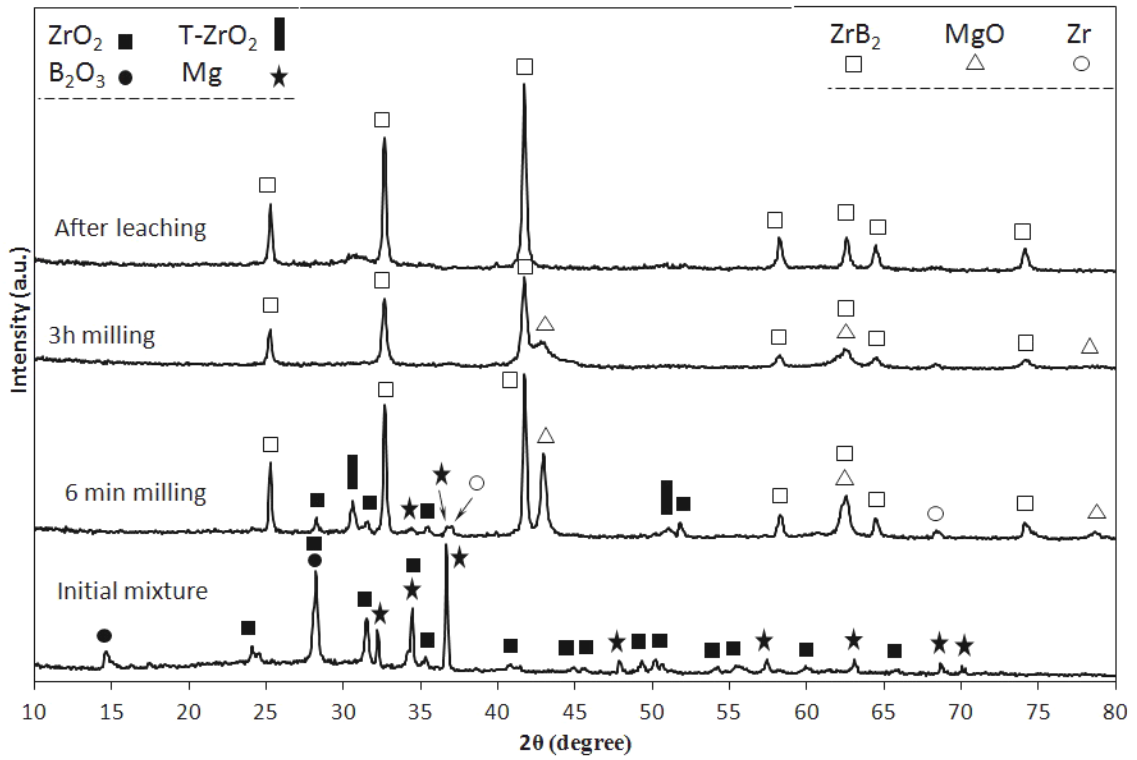


Fig. 2. X-ray diffraction patterns of the as-received, as-milled and leached samples of the Mg/ZrO<sub>2</sub>/B<sub>2</sub>O<sub>3</sub> system.

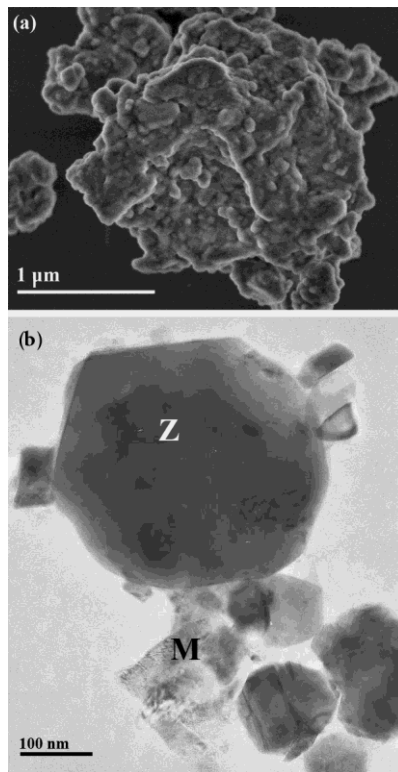


Fig. 3. (a) SEM and (b) TEM micrographs of the powder milled for 3 h.

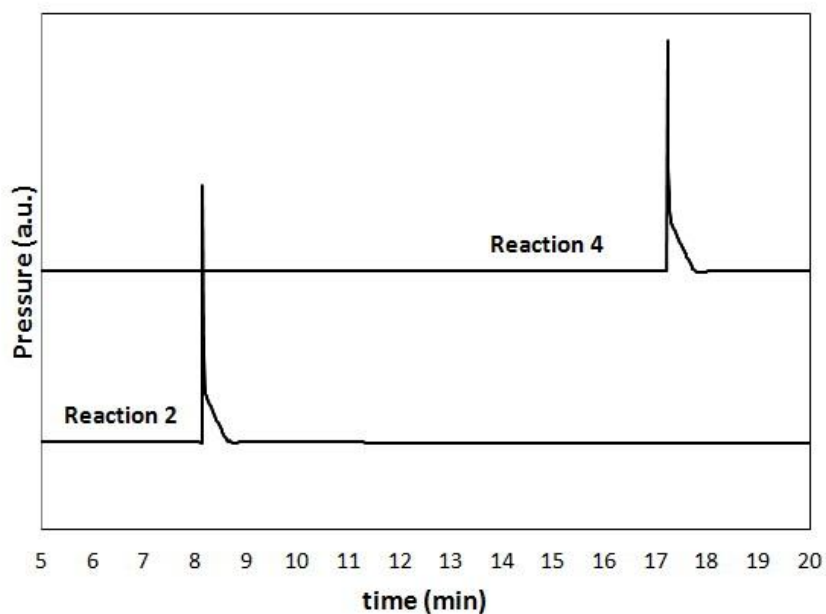


Fig. 4. Gas pressure inside the vial versus the milling time for the Mg/B<sub>2</sub>O<sub>3</sub> and Zr/B systems.

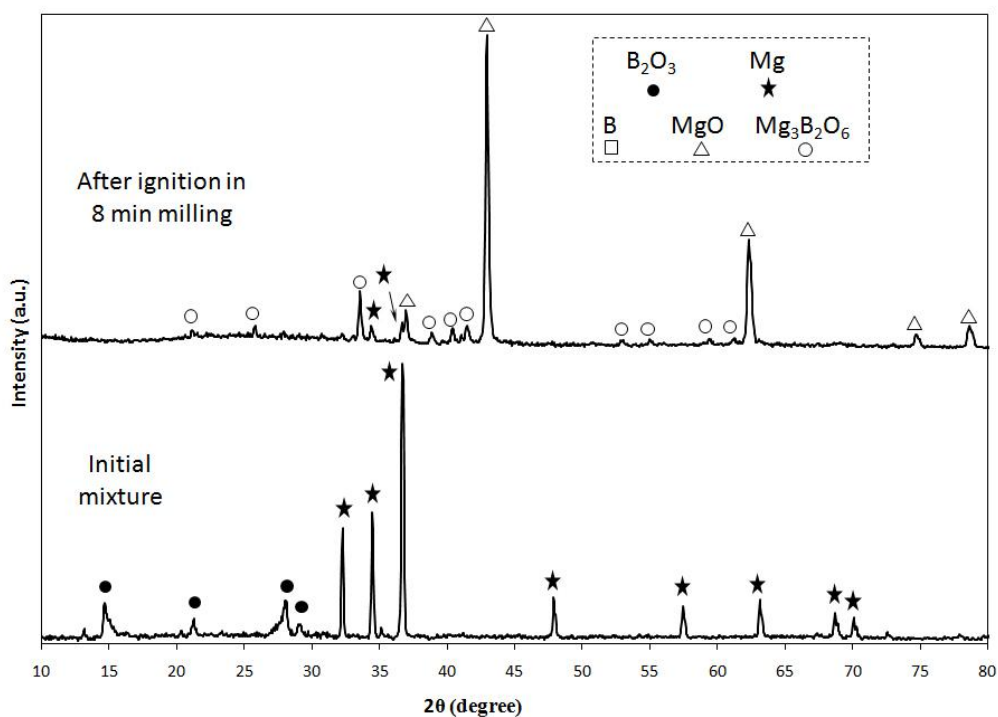


Fig. 5. X-ray diffraction patterns of the initial and the as-milled samples of the Mg/B<sub>2</sub>O<sub>3</sub> system.

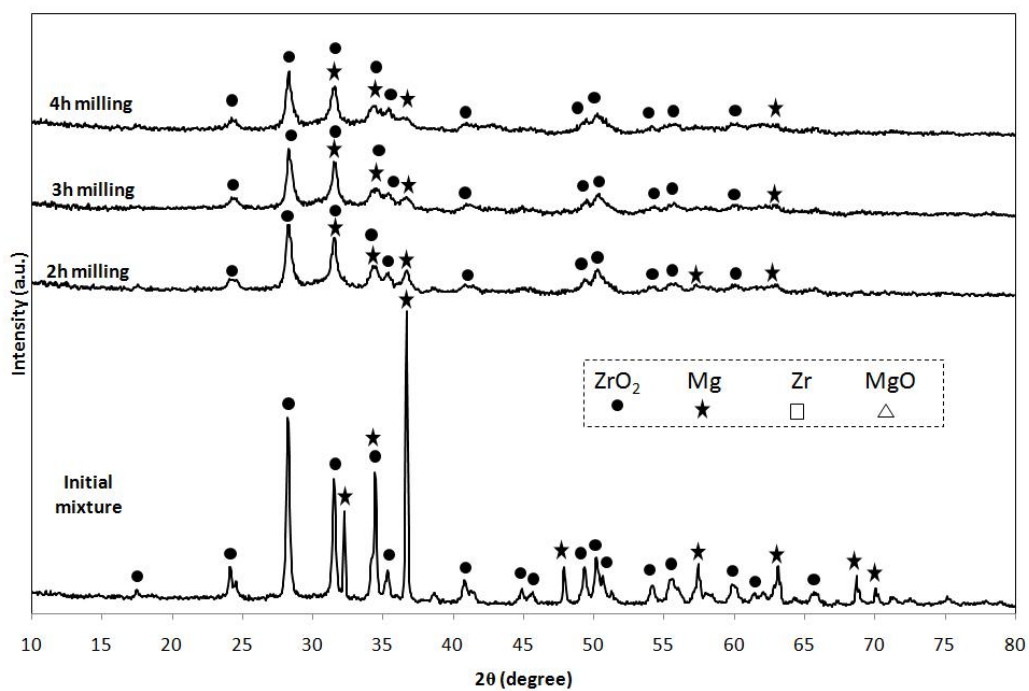


Fig. 6. X-ray diffraction patterns of the initial and the as-milled samples of the Mg/ZrO<sub>2</sub> system.

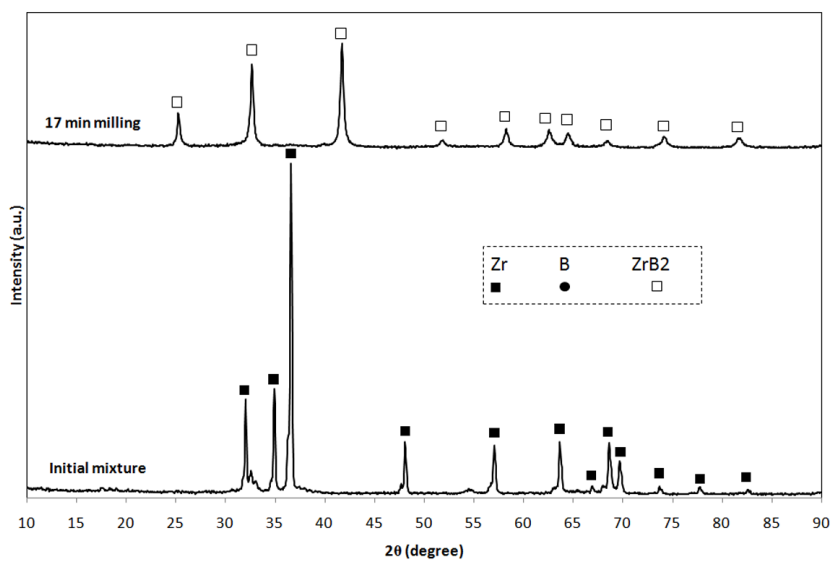


Fig. 7. X-ray diffraction patterns of the initial and the as-milled samples of the Zr/B system.

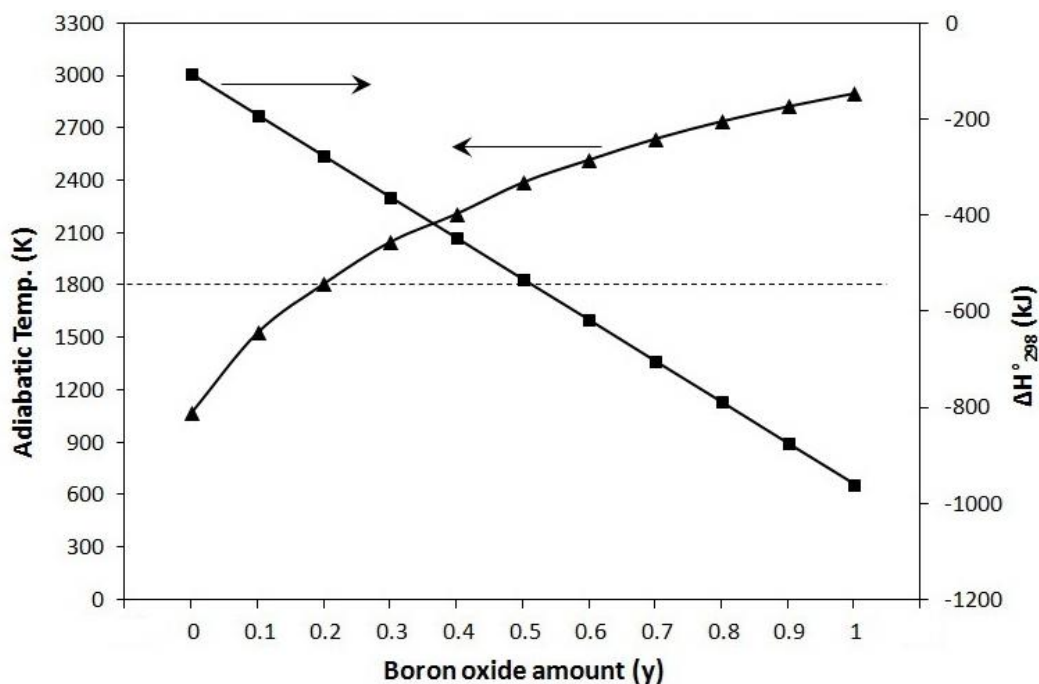


Fig. 8. Thermodynamic calculations of the adiabatic temperature and the room temperature enthalpy of reaction 5 versus the  $B_2O_3$  molar amount.

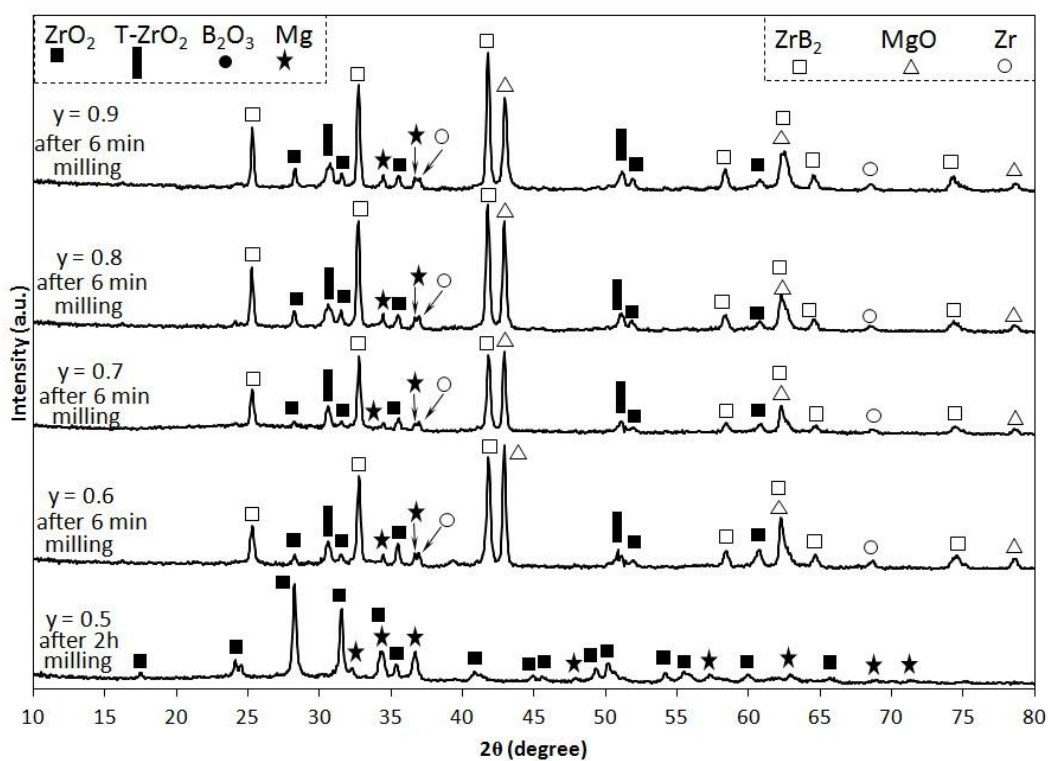


Fig. 9. X-ray diffraction patterns of the compositions of  $\gamma = 0.5-0.9$  in reaction 5 after milling.

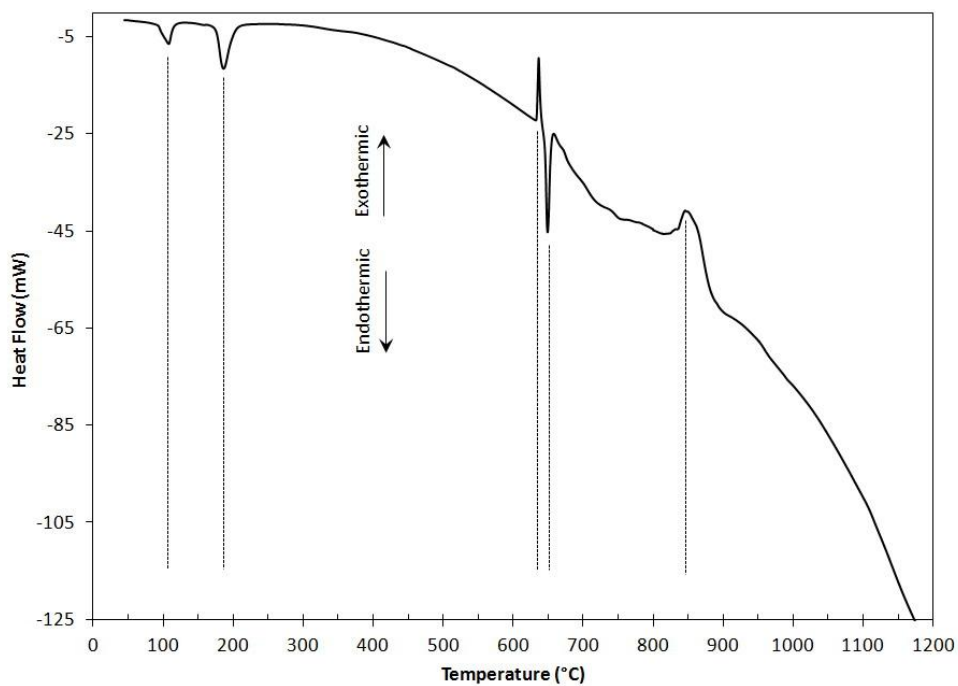


Fig. 10. DSC curve of the as-blended mixture of the Mg/ZrO<sub>2</sub>/B<sub>2</sub>O<sub>3</sub> system.

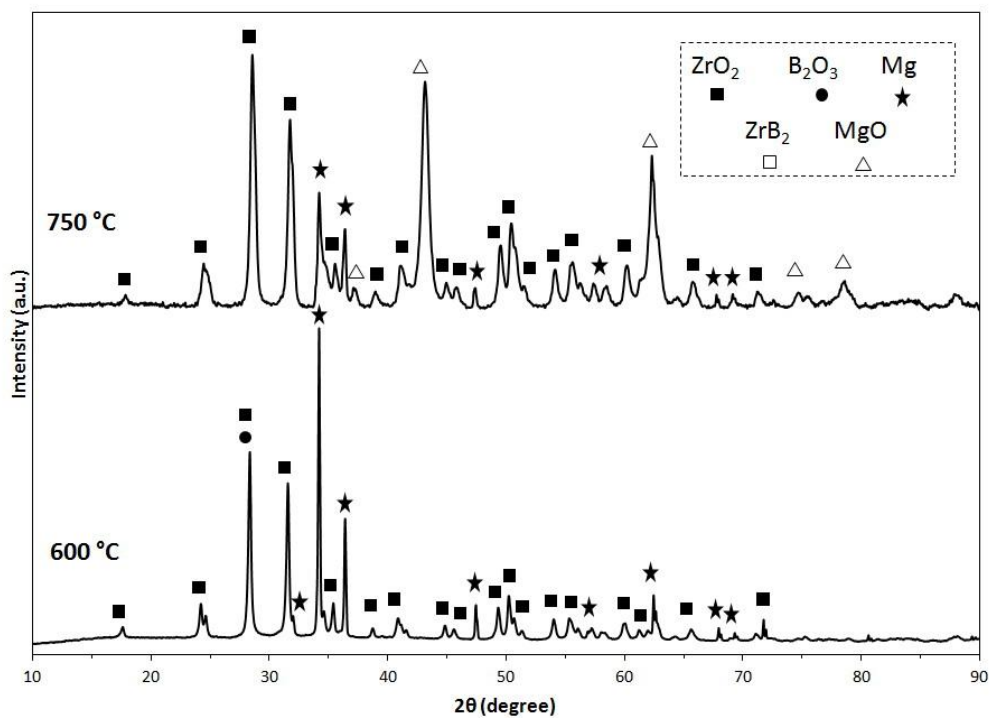


Fig. 11. X-ray diffraction patterns of the blended powders in the Mg/ZrO<sub>2</sub>/B<sub>2</sub>O<sub>3</sub> system after heating at 600 and 750°C (30 min dwell time at the maximum temperature, followed by cooling to room temperature).

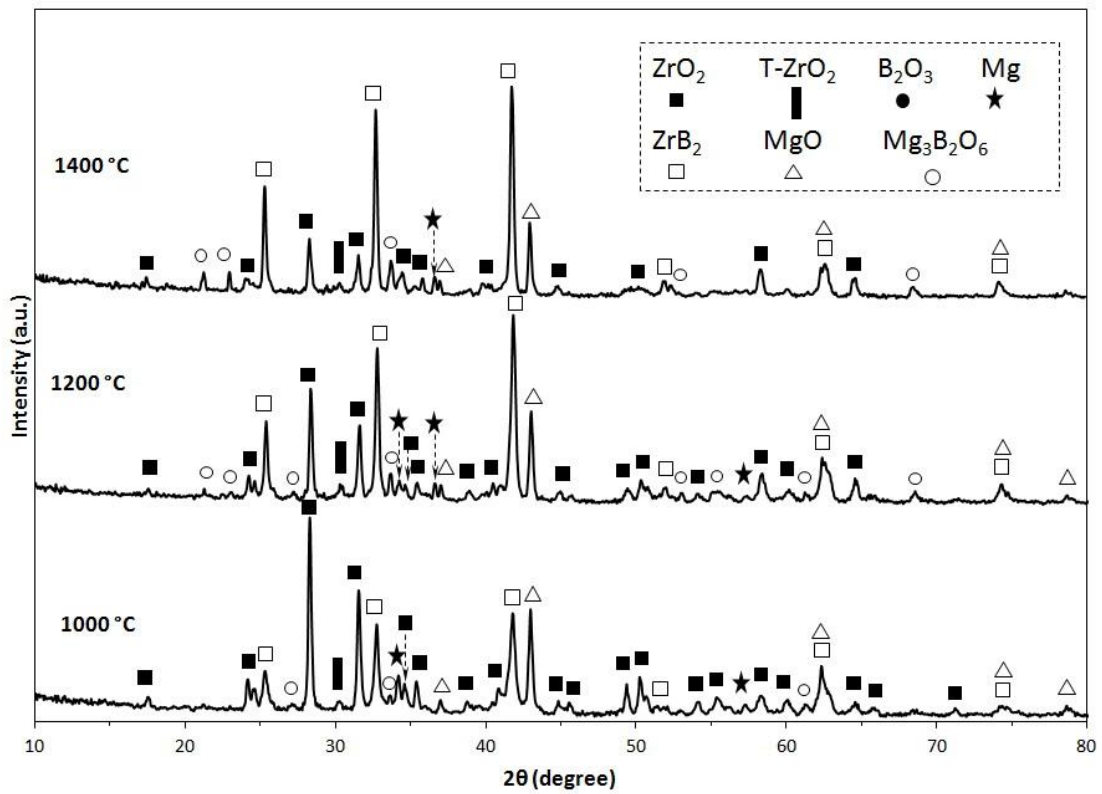


Fig. 12. X-ray diffraction patterns of the blended powders in the Mg/ZrO<sub>2</sub>/B<sub>2</sub>O<sub>3</sub> system after heating at 1000, 1200, and 1400 °C (30 min dwell time at the maximum temperature, followed by cooling to room temperature).